Published in final edited form as:
Biochemistry. 2013 March 19; 52(11): 1998–2006. doi:10.1021/bi400117q.

Identification of regions of rabbit muscle pyruvate kinase important for allosteric regulation by phenylalanine, detected by H/D exchange mass spectrometry†

Charulata B. Prasannan[a], **Maria T. Villar**[a], **Antonio Artigues**[a], and **Aron W. Fenton**[a,*]
[a]Department of Biochemistry and Molecular Biology, The University of Kansas Medical Center, MS 3030, 3901 Rainbow Boulevard, Kansas City, Kansas 66160

Abstract

Mass spectrometry has been used to determine the number of exchangeable backbone amide protons and the associated rate constants that are altered when rabbit muscle pyruvate kinase (rM_1-PYK) binds either the allosteric inhibitor (phenylalanine) or a non-allosteric analogue of the inhibitor. Alanine is used as the non-allosteric analogue since it binds competitively with phenylalanine, but elicits a negligible allosteric inhibition, i.e. a negligible reduction of the affinity of rM_1-PYK for the substrate, phosphoenolpyruvate (PEP). This experimental design is expected to distinguish changes in the protein caused by effector binding (i.e. those changes common upon the addition of alanine vs. phenylalanine) from changes associated with allosteric regulation (i.e. those elicited by the addition of phenylalanine binding, but not alanine binding). High quality peptic fragments covering 98% of the protein were identified. Changes in both the number of exchangeable protons per peptide and in the rate constant associated with exchange highlight regions of the protein with allosteric roles. The set of allosterically relevant peptides identified by this technique include residues previously identified by mutagenesis to have roles in the allosteric regulation by phenylalanine.

Pyruvate kinase catalyzes the final step in glycolysis, the transfer of phosphate from phosphoenolpyruvate to ADP to form pyruvate and ATP. Of the four mammalian isozymes, the one expressed in muscle tissue is commonly used as a model in studies of allosteric regulation. More specifically, the allosteric inhibition of rabbit muscle pyruvate kinase (rM_1-PYK) by phenylalanine has been extensively studied with a variety of biophysical techniques (1–15). Like other mammalian isozymes, rM_1-PYK is a homotetramer (15–21). Each subunit contains three domains, A, B, and C (Figure 1). Two types of interfaces are formed between subunits. The A-A interface primarily involves interactions between residues on two neighboring A domains and the C-C interface exclusively includes interactions between residues from two neighboring C domains. The active site lies between the A and B domains and the amino acid binding allosteric site lies between the A and C domains (16). The allosteric communication between these two sites occurs over a 40Å distance.

†This work was supported by NIH grant DK78076.

Corresponding authors: Aron W. Fenton, Department of Biochemistry and Molecular Biology, The University of Kansas Medical Center, MS 3030, 3901 Rainbow Boulevard, Kansas City, Kansas 66160, Phone: (913) 588-7033, Fax: (913) 588-9896, afenton@kumc.edu.

Supporting Information

Supporting information includes 1) replicate data for the free enzyme to evaluate error in parameter determination, 2) H/D exchange as a function of time for all peptides studied, 3) Fit parameters for H/D exchange for all peptides studied, and 4) a structural map of all areas of the protein NOT included in the phenylalanine vs. alanine comparison. This material is available free of charge via the internet at http://pubs.acs.org.

Despite biophysical characterization by numerous techniques, a detailed understanding of the allosteric mechanism of rM_1-PYK is still lacking. Our studies to address this knowledge gap have centered on defining allostery as how an enzyme binds a substrate in the presence vs. absence of an allosteric effector (22). Ideally, all four enzyme complexes in an allosteric energy cycle (free enzyme, enzyme-substrate complex, effector-enzyme complex and effector-enzyme-substrate ternary complex; (22)) should be characterized in a study of allostery (Figure 2A). Unfortunately the solubility limit of phenylalanine prevents studies of the ternary complex in the rM_1-PYK system (16, 23, 24). As an alternative approach to identify allosteric specific changes in the protein, we have developed a strategy to compare changes that result from binding of phenylalanine with those that result from the binding of alanine (22, 24) (Figure 2B). Alanine binds to rM_1-PYK competitively with phenylalanine (16). However, the impact of alanine binding on the protein's affinity for PEP is negligible. As such, alanine is treated as a non-allosteric analogue (i.e. alanine acts as X' in Figure 2) of the effector and any changes in the protein that result from alanine binding are considered important for effector binding only. In contrast, phenylalanine dependent changes must include both those important for effector binding and those that contribute to allostery. As such, those phenylalanine-dependent changes that are in addition to those caused by the binding of alanine are highlighted as important to allosteric function.

It has previously been proposed that protein changes in response to allosteric regulation include rotation of solid domains with respect to each other. This proposal was originally based on the change in small angle neutron scattering signatures that resulted from the addition of phenylalanine (5). Rotation-of-solid-domains was more generally supported for all allosteric mechanisms in PYK isozymes by comparisons of structures determined by X-ray crystallography (primarily among structures of different isozymes (25–27) and all in the absence of phenylalanine). We have recently challenged the rotation-of-solid-domains by demonstrating that changes in small angle X-ray scattering (SAXS) signatures are equivalent whether phenylalanine or alanine is added (28). The similarity in these responses is consistent with an interpretation that the large structural changes monitored by this moderate resolution technique is important to effector binding, but is not sufficient for allostery. However, our SAXS study did not clarify if allosteric specific changes were in addition to those associated with binding or if the two types of changes were completely independent. Nonetheless, none of the previously proposed mechanisms are completely consistent with available data, including that provided by our SAXS study.

As a first step in elucidating the allosteric mechanism of rM_1-PYK, we set a simple goal to identify regions of the protein that have altered properties as a result of allosteric regulation. Here we combine the phenylalanine vs. alanine comparison with mass spectrometry detection of hydrogen/deuterium exchange (H/DX-MS). H/DX-MS monitors changes in the amide linkages of the peptide backbone; side-chain hydrogen atoms exchange too rapidly to be monitored in the timescale of this measurement. We have not attempted to interpret whether changes are a result of conformational changes (i.e. the average of all conformations represented in the structural ensemble) or due to change in dynamics (frequency or amplitude) of protein motions. Instead, the phenylalanine vs. alanine comparison is only used to accomplish our simplistic goal of identifying regions of the protein that have altered properties as a result of allosteric regulation.

Materials and Methods

Materials

All chemical reagents were of analytical grade purchased from Sigma Chemical and Fisher Scientific. Rabbit muscle pyruvate kinase was purchased from (Roche) as an ammonium sulfate solution. Phenylalanine was purchased from Fluka, Biochimika. Alanine, 99% D_2O,

and trifluoroacetic acid were purchased from Sigma Chemical Co. Pepsin was purchased from Worthington. Mass spectrometric grade acetonitrile was from J.T. Baker Chemical.

Protein preparation

rM_1-PYK was desalted using G-50 resin in Tris/H_2O buffer (50 mM Tris-HCl, pH-9.0, 10 mM $MgCl_2$, 500 mM KCl, 0.1 mM EDTA). Protein concentration was determined based on absorbance at 280 nm and using the extinction coefficient of 29670 $cm^{-1}M^{-1}$ (or 0.54 mg^{-1} cm^{-1} mL) (29).

H/D exchange mass spectroscopic conditions

A rM_1-PYK stock solution was used to prepare 0.8mg/mL enzyme sample in Tris/D_2O buffer (50 mM Tris, measured pD= 8.59: equivalent to pH 9.0, 10 mM $MgCl_2$, 0.1 mM EDTA and 500 mM KCl) to contain 90% D_2O. The enzyme sample was incubated at 24°C. At various times of incubation, aliquots (10 KL) were removed and exchange was quenched by immediately adding cold ammonium phosphate buffer to result in a final pH of 2.4 at 0°C. Pepsin was added in 1:1 ratio (w/w) to the quenched sample for proteolytic cleavage. This cleavage reaction was incubated for 2.5 minutes before separating peptides on a C-18 HPLC column. The resulting peptides were analyzed by on-line HPLC Tandem mass spectrometry.

Tandem mass spectrometry

Peptide identification was performed using nondeuterated protein (control samples). Following peptic digestion as indicated above, the resulting peptic peptides were loaded on a reverse phase C18 column (Zorbax C18SB, 1cm × .32 mm, 300 μm, MicroTech Scientific) and desalted for 2.5 min at 75 Kl/min with solvent A (0.05% TFA). Then peptides were eluted with the following gradient: 20% to 60% solvent B (0.05% TFA in acetonitrile) in 6 min., followed by a 60% to 80% solvent B in 1 min. and a wash at 80% solvent B for 5 min. Finally the column was pre-equilibrated with solvent A for 7 min., before injection of the next sample. The peptic peptides eluted from the column between 5 and 15 minutes. Peptide desalting and separation were performed at −2°C, using a custom build cooling chamber, SAIDE interface, which consistently reduces back exchange to 17% (30). The mass spectrometer (LTQ FT, ThermoFinnigan) was operated in data-dependent mode to perform one MS scan on the FT at a resolution of 50,000 for an ion of m/z of 400, followed by 6 MS2 scans on the six most intense ions on the ion trap using an exclusion list and a repeat of 1. To obtain full coverage of the protein amino acid sequence by multiple overlapping peptides, several rounds of HPLC MS/MS were required. For each successive scan an exclusion list was built by searching a protein database as indicated below. The identified peptide-ions were included in the exclusion list to reject those peptide ions that have been identified on previous rounds.

For peptide identification, all data were analyzed using the Sequest algorithm (31) included in the BioWorks Browser package (Version 3.1, ThermoFinnigan). Data were used to search a protein database containing the amino acid sequences of rM_1-PYK and porcine pepsin. The following specifications were included: 1) no enzyme specificity for the protease, 2) a parent ion tolerance of 20 ppm and 3) a fragment ion tolerance of 0.3 Da. The identified peptides were then filtered using the following set of criteria: 1) a Xcorr score equal to or higher than 1.5, 2, or 2.5 for ions with z equal to 1, 2 or 3, respectively and 2) a minimum deltaCorr score of 0.08. Similar procedure was used for deuterated samples, with the only difference being that no tandem mass analysis was performed; i.e. only survey scans on the ICR FT were used at identical resolution.

We obtained 98% coverage of the protein. These peptides obtained were small and overlapping which are ideal for the rate calculations in the H/D exchange experiments (32–34). Note that this total number of peptides could not be analyzed for all enzyme complexes included in this study. However, the final comparison between the alanine-bound complex vs. the phenylalanine-bound complex included data for 74% of the protein (see Supplemental Material).

Measurement of deuterium content

H/D exchange data obtained for rM_1-PYK enzyme was analyzed using 3 different approaches: HDXfinder (35); HDExaminer (Sierra Analytics); and manual analysis using Qual Browser (Thermo-Finnigan) and Mag-Tran (36). Outputs from all three approaches were combined to maximize the number of peptides identified. When the same peptide was analyzed by the three methods, similar data were obtained (data not shown). For all analysis approaches, at a given time (t), the number of deuterium incorporation (D_t) is calculated by

$$D_t = \frac{M_t - M_0}{[\Delta D]} \times z, \quad (1)$$

where M_t is the total mass observed for a peptide at a given time, M_0 is the mass obtained for peptide in the unlabeled sample, $[\Delta D]$ is the mass difference of deuterium relative to hydrogen, and z is the charge of the peptide.

For most of the peptides we observed two phases of exchange, a fast exchange and a slow exchange. Therefore deuterium content of a peptide at various times was fit to:

$$D = N_1(1 - \exp^{-k_1 t}) + N_2(1 - \exp^{-k_2 t}), \quad (2)$$

where D is the deuterium content at time t, N_1 and N_2 are the number of fast and slow exchanging amide atoms, and k_1 and k_2 are the respective rate constants. Equation 2 was used in Kaleidagraph (Synergy software) to obtain the rate of exchange for the fast and the slow phases. Due to limited data defining the fast phase, only the rates for the slow phase were used for comparisons in this study. For any one peptide, the total amount of deuterium was calculated as a sum of N_1 and N_2 from equation 2.

Results

Data Analysis

Figure 3 shows example data sets comparing the exchange as a function of time. Each panel represents a comparison of the response of one peptide. In each panel, data for the free enzyme are in green, data for the alanine-bound complex are in blue, and data for the phenylalanine-bound complex are in red. Visual inspection for the examples in Figure 3 confirms that peptide exchange as a function of time can be fit to two rates, a finding that is consistent for most peptides included in this study (see Supplemental Material for exceptions). Each of the two rates for any one peptide is associated with a number of proton exchanges. Due to the selection of times used for data collection, very little information is available for determining the rate in the faster of the two exchange rates for any one peptide. Only the addition of quench flow (not currently available in our laboratory) will allow a more thorough characterization of the fast rate of exchange. Due to limited definition of the fast rate, the current study only compares changes in the slower rates of exchange. This is in addition to the comparison of the total number of exchangeable protons per peptide.

The three panels in Figure 3 represent three different examples of responses that result from ligand binding. In panel A, binding of alanine or phenylalanine causes no change in the

number of exchangeable protons on the representative peptide and no change in the rate of proton exchange (comparisons with respect to the free enzyme). Panel B shows a representative peptide that shows a different number of exchangeable protons depending on the enzyme complex analyzed. In this second example, the peptide from the phenylalanine-bound complex, the alanine-bound complex and the free enzyme have 6, 4, and 3 exchangeable protons, respectively. Finally, Panel C shows an example peptide that does not experience a ligand-dependent change in the number of exchangeable protons, but instead has a ligand-dependent change in the exchange rate. These three peptides then exemplify the type of responses obtained in this study. All time dependent exchanges for peptides for the three enzyme complexes (free enzyme, alanine-bound, and phenylalanine-bound) are included in the supplemental material.

We initiated analysis of the data by contrasting alanine induced changes (free enzyme vs. alanine-bound complex) with phenylalanine induced changes (free enzyme vs. phenylalanine-bound complex). Of course the differences between these two sets of changes is equivalent to those identified by directly comparing peptides obtained from the alanine-bound complex with those from the phenylalanine-bound complex. Therefore, peptides obtained for these two complexes, which are not also present in the free enzyme were useful for our comparison. For those peptides that could be compared (74% of the protein), differences between the number of exchangeable protons and the differences between the rate of exchange were mapped onto the structure of rM_1-PYK (detailed below). To graphically represent changes in the total number of exchangeable protons, these changes were binned for peptides that include a change in one (blue), two (purple) or more (red) exchangeable protons (See Figure 4 below). Changes in rate constants that exceeded the 8% cutoff determined by our error estimate were first converted to relative rate change (i.e. $\frac{\text{(rate of peptide from complex 1)} - \text{(rate of peptide from complex 2)}}{\text{(rate of peptide from complex 2)}}$). Relative rate changes for each peptide were then scaled to the largest relative rate change identified when comparing the phenylalanine-bound and alanine-bound complexes (both increases and decreases scaled to same maximum change). This standardized relative rate change was then color coded with a gradient (See Figure 5 below). The white to red gradient reflects changes that increase in rate and the white to blue gradient (not perceptible in figures) reflects changes that decrease in rate.

Data Reproducibility and Controls

We have previously shown that allosteric regulation of rM_1-PYK by phenylalanine functions in D_2O (23). Although the retention of function in D_2O may be an obvious control for any study using H/D exchange, this control has not been included in several H/DX-MS studies of allostery reported in the literature. We previously used the phenylalanine regulation of rM_1-PYK as an example of this control. Although phenylalanine affinity is reduced in the presence of D_2O, this inhibitor continues to reduce PEP affinity in this alternative solvent.

To obtain a complete characterization of the allosteric regulation of rM_1-PYK by phenylalanine, our design was to compare the extent of H/D exchange and the rate constants for this exchange over the complete protein primary sequence, in the free and the bound states as indicated above. However, the determination of exchange rates requires considerably more data collection (1978 individual peptide mass measurements are included in this study) than would be required for a simpler study focusing only on the number of exchangeable protons. This need for an increased data set limits the feasibility of replicates of individual data sets. As a result two controls were included to confirm data reproducibility.

First, detection of the total number of exchangeable protons in the protein was replicated for each complex studied. The full length rM_1-PYK protein does not tolerate standard conditions used for protein desalting by reverse phase analysis on C3, C4, or C8 columns. Such desalting results in protein aggregation, preventing analysis of total number of exchangeable protons by measuring the change in mass of the intact protein during H/D exchange conditions. As an alternative, a sum of exchangeable protons (i.e. N1 and N2 values from fits to Eq 2) for all non-overlapping peptides was used. The free enzyme, the phenylalanine-bound complex and the alanine-bound complex have 139, 150, and 151 exchangeable protons in a set of peptides. To confirm reproducibility of these values, each complex was analyzed independently after 24 hrs of exchange. Based on the mass vs. time data (below), 24 hrs should allow exchange to reach equilibrium and the number of exchanges at this time should reflect the totals determined from the fitting approach just described. The exchangeable protons in this replicate data for the same set of peptides are 139, 146, and 146 for the free enzyme, the phenylalanine-bound complex and the alanine-bound complex, respectively. Therefore, this data indicates the number of exchangeable protons can be determined with approximately 2% error.

As a second control, reproducibility of rate constants obtained from mass vs. time data was confirmed by obtaining replicate data for the free enzyme. For peptides included in Supplemental Figure 1, similar rates were obtained from the two independent data sets. Comparing these two data sets, the average error in the total number of exchangeable protons was 1%, which compares well with the 2% error determined above. In addition, the average relative standard deviation between the rate constants determined from the two data sets was 8%. As a result, only changes in rate constants that exceed 8% difference are considered in comparisons.

Protons protected/deprotected due to effector binding and/or allostery

This work focuses on the use of a “non-allosteric analogue” (i.e. alanine) as a comparison to distinguish changes in the protein that are uniquely important to allostery, as opposed to assigning allosteric roles to all effector-induced changes in the protein. The benefit of this comparison becomes immediately obvious upon comparing the peptide locations of protons that are completely protected/deprotected upon effector binding (Figure 4). Figure 4A highlights all peptides with alanine-dependent changes in the total number of exchangeable protons. Figure 4B shows the equivalent data that result from the binding of phenylalanine. Overall, the pattern of changes caused by the binding of these two effectors is very similar. However, once the changes elicited by the binding of alanine are subtracted from those changes caused by the binding of phenylalanine (and considering overlapping peptides to identify the smallest “unit containing exchangeable protons; see supplemental material), only a few areas of the protein are highlighted for roles in allostery (Figure 4C). As one particular example, consider the α-helix colored in blue and marked by an asterisk (*: peptide 215–237) in Figure 4A and 4B. This peptide is highlighted due to a change in the protection against exchange that results from binding of a ligand in the effector binding site. However, this ligand-dependent change is equivalent whether the ligand does, or does not elicit a change in the affinity of the protein for its substrate. Therefore, this change is most likely related to effector binding instead of being specific to allosteric functions and there is no difference highlighted for this region in Figure 4C. Also, for a few peptides (e.g. the one marked with # is 468–485) the error of the difference when comparing two complexes dismissed the difference from further consideration; the example peptide 468–485 shows a slightly significant difference in a comparison of the phenylalanine-complex with the free enzyme (# in 4B), but does not have a significant difference when comparing the alanine-complex with the free enzyme (# in 4A). Therefore the visual difference between panel A and B does not necessarily result in the same peptide being highlighted in panel C.

In the alanine-bound complex vs. phenylalanine-bound complex comparison (Figure 4C), overlapping peptides were compared to identify the smallest sequence "unit" (smaller than peptides detected; see Supplemental Figure S10) containing exchangeable protons. There are four such regions. What is lost in the color coding used in Figure 4C is the quantitative nature of the differences between exchange in the alanine-complex compared to that in the phenylalanine-complex. 156–158 is more protected in the phenylalanine-complex as compared to the alanine-complex. Interestingly, there is no direct evidence for this phenylalanine-dependent protection at the peptide level. Instead the protection of this B-domain "unit" is assigned based on a comparison of the 157–179 and the 154–179 peptide. Since the longer peptide displays less change when comparing the two complexes, the extra length in the 154–179 peptide must contain a region that is more protected in the phenyalanine complex. As stated elsewhere, the first two amino acids of any peptide experience back-exchange that is too fast to be detected (38). Therefore, the difference between these two peptides is assigned to 156–158. In contrast to the added protection in the 156–159 unit, the neighboring 159–160 "unit" in the B-domain, includes two residues that experience more exchange in the phenyalanine-complex compared to that in the alanine-complex. The 372–378 peptide in the A-domain is also less protected against exchange in the phenyalalnine-complex, but the 428–430 in the C-domain is more protected in the phenylalnine-complex.

Peptides with altered rates of exchange due to effector binding/allostery

It is not uncommon for H/DX-MS studies to focus only on changes in the number of exchangeable protons, and this approach can be very informative (39, 40). However, rates of exchange contain a wealth of information that is not detected in a more restricted study of total number of exchangeable protons. Several studies have already used H/DX-MS to determine rates of exchange in allosteric systems (41–46). We also used rates of exchange at peptide resolution in this study. The rate constants for these exchange events were compared for the free enzyme, the alanine-bound complex, and the phenylalanine-bound complex (Figure 5).

Upon alanine binding there are notably few changes in rate constants (Figure 5A). Interestingly, all notable changes result in increased rates of exchange. Binding of phenylalanine (Figure 5B) causes more changes than alanine binding. Again, these changes are exclusively increases in exchange rates compared to the free enzyme. Figure 5C, shows the relative rate changes that are present when phenylalanine is bound compared to when alanine is bound. All notable changes are a result of phenylalanine causing rates of exchange to increase relative to rates of exchange in the alanine-bound complex. Overall the areas of the protein identified for roles in allostery by comparing rates of exchange (Figure 5C) are in the same general region of the protein as those identified by comparing the total exchange (Figure 4C).

Combining Figures 4C and 5C (see Figure 6) indicates that an area of the A-domain and areas surrounding the active site for roles in the allosteric mechanism. However, it is interesting to note that none of the highlighted areas near the active site contain residues that actually make direct contact with PEP. More expectedly, the areas highlighted for roles in allostery include peptides that contain residues in the amino acid effector binding site. In fact, all residues in this binding site are included in peptide comparisons between the alanine-bound vs. phenylalanine-bound complexes. Of these effector binding site residues, Arg42, Asn43, and Asn69 are included in peptides highlighted for roles in allostery. In contrast, peptides including effector site residues Arg105, His463, Pro470, Ile468, and Phe469 were not highlighted for roles in allostery. We can then speculate that when the phenylalanine effector molecule binds in this binding site, rearrangements of residues Arg42, Asn43, and Asn69 are key to eliciting the allosteric response.

Discussion

As outlined in the introduction, H/D exchange was used to detect solvent accessibility when rM_1-PYK binds either phenylalanine or alanine. Changes identified when phenylalanine binds, which are in addition to those change induced by alanine binding, are considered important for allosteric regulation. Several caveats should be acknowledged in this approach. First, this comparative approach is not expected to identify allosterically relevant changes that are dependent on the presence of the substrate (i.e. those represented in the two complexes on the right hand side of Figure 2A). The basis of this consideration has been illustrated in detail elsewhere (22). Second, H/DX-MS only detects exchange in the backbone amide groups and does not report on changes located in side-chains. Third, due to the focus on changes in solvent accessibility, changes that are buried in the hydrophobic core with no access to solvent under any of the liganded states will not be reported; i.e. even though the peptide mass maps show high coverage of the protein, only a fraction of amides included on any one peptide experiences exchange. Fourth, all changes must be considered as an average across all four subunits in a tetramer. Ligand concentrations have been selected to saturate the effector binding site and prevent the introduction of asymmetry into the protein (i.e. only a fraction of the effector binding sites being filled during characterization). However, there remains the potential for half-site-reactivity type mechanisms (47, 48) that would not be detected due to the averaging effect. Fifth, it is not clear how much change in the rate of exchange is necessary to impact the free energy of allostery. Therefore, even though we focus on larger rate changes, the areas with more subtle changes may play very important roles in the allosteric mechanism. Finally, the data are collected at peptide resolution, not at amino acid resolution. This final caveat should be considered while viewing color coded structures in Figures 4–6. Any highlighted region of the protein may appear to include a large area of the protein, when the changes of interest may in reality be localized at a single amide.

Despite these caveats, the advantage of the current study is the simple experimental design to compare the changes that occur upon binding of a non-allosteric effector (alanine) vs. binding of the allosteric effector (phenylalanine) as a means of identifying allosterically relevant changes in rM_1-PYK. When combining all changes identified with allosteric relevance (Figure 6), most changes highlighted are in the A-domain and surrounding the active site. This overall finding is interesting given that they were identified by contrasting the influence of ligand binding at the allosteric site.

There are relatively few mutational studies of rM_1-PYK that include characterization of inhibition by phenylalanine. Mutations introduced into rM_1-PYK have been designed either based on mutations identified in non-spherocytic anemia (1) or based on differences between the M_1- and M_2-PYK isozymes (7, 49, 50). However, most of these mutations have been characterized to determine the influence on regulation by Fru-1,6-BP activation. Only four (T340M, R119C, Q377K, A398R) have been characterized for the impact on inhibition by phenylalanine (1, 49). Some property of phenylalanine inhibition was indicated to be altered for T340M, Q377K, and A398R. Of these, we did not observe a peptide that included A398. However, T340 and Q377 are located on “units” highlighted in this study for changes associated with allostery (Figure 6). Therefore, the locations of identified regions in this study are consistent with previously reported functional characterizations of phenylalanine inhibition of rM_1-PYK.

Interestingly, of the area in the C-C domain interface that contains the 22 amino acid differences between the M_1- and M_2-PYK isozymes only the 426–428 peptide is highlighted as an area of the protein influenced by phenylalanine regulation. As a review, the M_2-PYK, but not the M_1-PYK, is activated by fructose-1,6-bisophosphate. This altered response must

be directly mediated by the 22 amino acid differences that reside in the C-C interface. Therefore, within the context of a two-state (i.e. R to T transition) model of allostery the lack of detection of allosteric specific changes within the C-C domain interface may be a surprise; in a two-state mechanism, all forms of cooperativity in ligand binding and heterotropic allostery must of necessity be interdependent. However, as previously discussed in detail (21) a linked-function view of allostery allows each effector to modify the affinity of the substrate independently. Based on this second view of allostery and since the studies described here focus on regulation by the amino acid inhibitor, there is no expectation that regions of the protein important to regulation by fructose-1,6-bisphosphate should be identified. Therefore, the fact that we identify only a very small region of the protein that are different between the M_1- and M_2-PYK isozymes is consistent with the both proteins being inhibited by phenylalanine.

Although the use of H/DX-MS reported here does not offer insights into the regulation of M_1-PYK by fructose-1,6-bisophosphate, we cannot completely disregard the role of the 426–428 region when considering regulation by phenylalanine. Although both M_1-PYK and M_2-PYK allosterically share a response to phenylalanine from a qualitative perspective, they do not share qualitative aspects of this regulation (e.g. altered affinity for PEP, altered affinity for phenylalanine, and/or a slightly different extent of allosteric coupling between the binding of these two ligands). Therefore, it seems very likely that this 436–428 region may contribute to these unique features in the two highly similar isozymes.

Also of interest, regions on the outside of the protein have been highlighted for a role in allostery. This final observation likely reflects the bias of H/DX-MS that is dependent on solvent accessibility. However, it serves as a reminder that allostery is not necessarily restricted to changes in the hydrophobic core, a misconception that might be conceived due to the equally biased detection approach of methyl labeling NMR measurements of dynamics (51–53); the complementary nature of H/DX-MS and methyl labeling NMR is, however, very promising.

In conclusion, we have used H/DX-MS to identify regions of the protein that experience change in solvent accessibility upon binding of effector. These changes have been further subdivided to identify areas of the protein with functions in the allosteric mechanism by comparing change induced by binding of the allosteric effector that are in addition to changes caused by the binding of a non-allosteric effector analogue. The highlighted areas are consistent with other available, albeit limited, data in the literature. This use of non-allosteric effector analogues may be a generally applied technique to tease out changes in proteins that are specifically important to allosteric functions.

Supplementary Material

Refer to Web version on PubMed Central for supplementary material.

Abbreviations

PYK	pyruvate kinase
rM_1-PYK	the pyruvate kinase isozyme found in rabbit brain and muscle
PEP	phosphoenolpyruvate

References

1. Cheng X, Friesen RH, Lee JC. Effects of conserved residues on the regulation of rabbit muscle pyruvate kinase. J Biol Chem. 1996; 271:6313–6321. [PubMed: 8626426]
2. Consler TG, Jennewein MJ, Cai GZ, Lee JC. Synergistic effects of proton and phenylalanine on the regulation of muscle pyruvate kinase. Biochemistry. 1990; 29:10765–10771. [PubMed: 2176882]
3. Consler TG, Jennewein MJ, Cai GZ, Lee JC. Energetics of allosteric regulation in muscle pyruvate kinase. Biochemistry. 1992; 31:7870–7878. [PubMed: 1510974]
4. Consler TG, Lee JC. Domain interaction in rabbit muscle pyruvate kinaseIEffects of ligands on protein denaturation induced by guanidine hydrochloride. J Biol Chem. 1988; 263:2787–2793. [PubMed: 3343232]
5. Consler TG, Uberbacher EC, Bunick GJ, Liebman MN, Lee JC. Domain interaction in rabbit muscle pyruvate kinase. II. Small angle neutron scattering and computer simulation. J Biol Chem. 1988; 263:2794–2801. [PubMed: 3343233]
6. Consler TG, Woodard SH, Lee JC. Effects of primary sequence differences on the global structure and function of an enzyme: a study of pyruvate kinase isozymes. Biochemistry. 1989; 28:8756–8764. [PubMed: 2605219]
7. Friesen RH, Castellani RJ, Lee JC, Braun W. Allostery in rabbit pyruvate kinase: development of a strategy to elucidate the mechanism. Biochemistry. 1998; 37:15266–15276. [PubMed: 9799487]
8. Friesen RH, Chin AJ, Ledman DW, Lee JC. Interfacial communications in recombinant rabbit kidney pyruvate kinase. Biochemistry. 1998; 37:2949–2960. [PubMed: 9485447]
9. Friesen RH, Lee JC. The negative dominant effects of T340M mutation on mammalian pyruvate kinase. J Biol Chem. 1998; 273:14772–14779. [PubMed: 9614077]
10. Heyduk E, Heyduk T, Lee JC. Global conformational changes in allosteric proteins. A study of Escherichia coli cAMP receptor protein and muscle pyruvate kinase. J Biol Chem. 1992; 267:3200–3204. [PubMed: 1737775]
11. Oberfelder RW, Barisas BG, Lee JC. Thermodynamic linkages in rabbit muscle pyruvate kinase: analysis of experimental data by a two-state model. Biochemistry. 1984; 23:3822–3826. [PubMed: 6487577]
12. Oberfelder RW, Consler TG, Lee JC. Measurement of changes of hydrodynamic properties by sedimentation. Methods Enzymol. 1985; 117:27–40. [PubMed: 4079807]
13. Oberfelder RW, Lee JC. Measurement of ligand-protein interaction by electrophoretic and spectroscopic techniques. Methods Enzymol. 1985; 117:381–399. [PubMed: 4079810]
14. Oberfelder RW, Lee LL, Lee JC. Thermodynamic linkages in rabbit muscle pyruvate kinase: kinetic, equilibrium, and structural studies. Biochemistry. 1984; 23:3813–3821. [PubMed: 6487576]
15. Wooll JO, Friesen RH, White MA, Watowich SJ, Fox RO, Lee JC, Czerwinski EW. Structural and functional linkages between subunit interfaces in mammalian pyruvate kinase. J Mol Biol. 2001; 312:525–540. [PubMed: 11563914]
16. Williams R, Holyoak T, McDonald G, Gui C, Fenton AW. Differentiating a Ligand's Chemical Requirements for Allosteric Interactions from Those for Protein Binding. Phenylalanine Inhibition of Pyruvate Kinase. Biochemistry. 2006; 45:5421–5429. [PubMed: 16634623]
17. Larsen TM, Benning MM, Rayment I, Reed GH. Structure of the bis(Mg2+)-ATP-oxalate complex of the rabbit muscle pyruvate kinase at 2.1 A resolution: ATP binding over a barrel. Biochemistry. 1998; 37:6247–6255. [PubMed: 9572839]
18. Larsen TM, Benning MM, Wesenberg GE, Rayment I, Reed GH. Ligand-induced domain movement in pyruvate kinase: structure of the enzyme from rabbit muscle with Mg2+, K+, and L-phospholactate at 2.7 A resolution. Arch Biochem Biophys. 1997; 345:199–206. [PubMed: 9308890]
19. Larsen TM, Laughlin LT, Holden HM, Rayment I, Reed GH. Structure of rabbit muscle pyruvate kinase complexed with Mn2+, K+, and pyruvate. Biochemistry. 1994; 33:6301–6309. [PubMed: 8193145]
20. Stuart DI, Levine M, Muirhead H, Stammers DK. Crystal structure of cat muscle pyruvate kinase at a resolution of 2.6 A. J Mol Biol. 1979; 134:109–142. [PubMed: 537059]

21. Fenton AW, Johnson TA, Holyoak T. The pyruvate kinase model system, a cautionary tale for the use of osmolyte perturbations to support conformational equilibria in allostery. Protein Sci. 2010; 19:1796–1800. [PubMed: 20629175]
22. Fenton AW. Allostery: an illustrated definition for the 'second secret of life'. Trends Biochem Sci. 2008; 33:420–425. [PubMed: 18706817]
23. Prasannan CB, Artigues A, Fenton AW. Monitoring allostery in D2O: a necessary control in studies using hydrogen/deuterium exchange to characterize allosteric regulation. Anal Bioanal Chem. 2011; 401:1083–1086. [PubMed: 21701851]
24. Fenton AW, Reinhart GD. Isolation of a single activating allosteric interaction in phosphofructokinase from Escherichia coli. Biochemistry. 2002; 41:13410–13416. [PubMed: 12416986]
25. Valentini G, Chiarelli LR, Fortin R, Dolzan M, Galizzi A, Abraham DJ, Wang C, Bianchi P, Zanella A, Mattevi A. Structure and function of human erythrocyte pyruvate kinase. Molecular basis of nonspherocytic hemolytic anemia. J Biol Chem. 2002; 277:23807–23814. [PubMed: 11960989]
26. Rigden DJ, Phillips SE, Michels PA, Fothergill-Gilmore LA. The structure of pyruvate kinase from Leishmania mexicana reveals details of the allosteric transition and unusual effector specificity. J Mol Biol. 1999; 291:615–635. [PubMed: 10448041]
27. Jurica MS, Mesecar A, Heath PJ, Shi W, Nowak T, Stoddard BL. The allosteric regulation of pyruvate kinase by fructose-1,6-bisphosphate. Structure. 1998; 6:195–210. [PubMed: 9519410]
28. Fenton AW, Williams R, Trewhella J. Changes in small-angle X-ray scattering parameters observed upon binding of ligand to rabbit muscle pyruvate kinase are not correlated with allosteric transitions. Biochemistry. 2010; 49:7202–7209. [PubMed: 20712377]
29. Boyer, PD. Pyruvate Kinase. In: Boyer, PD.; Lardy, HA.; Myrback, K., editors. The Enzymes. 2nd Edition ed.. Academic Press; New York: 1962. p. 95-113.
30. Villar MT, Miller DE, Fenton AW, Artigues A. SAIDE: A Semi-Automated Interface for Hydrogen/Deuterium Exchange Mass Spectrometry. Proteomica. 2010; 6:63–69.
31. Eng JK, McCormack AL, Yates JR. An approach to correlate tandem mass spectral data of peptides with amino acid sequences in a protein database. Journal of the American Society for Mass Spectrometry. 1994; 5:976–989.
32. Rosa JJ, Richards FM. An experimental procedure for increasing the structural resolution of chemical hydrogen-exchange measurements on proteins: application to ribonuclease S peptide. J Mol Biol. 1979; 133:399–416. [PubMed: 43900]
33. Englander SW, Kallenbach NR. Hydrogen exchange and structural dynamics of proteins and nucleic acids. Q Rev Biophys. 1983; 16:521–655. [PubMed: 6204354]
34. Zhang Z, Smith DL. Determination of amide hydrogen exchange by mass spectrometry: a new tool for protein structure elucidation. Protein Sci. 1993; 2:522–531. [PubMed: 8390883]
35. Miller DE, Prasannan CB, Villar MT, Fenton AW, Artigues A. HDXFinder: Automated Analysis and Data Reporting of Deuterium/Hydrogen Exchange Mass Spectrometry. J Am Soc Mass Spectrom. 2011
36. Zhang Z, Marshall AG. A universal algorithm for fast and automated charge state deconvolution of electrospray mass-to-charge ratio spectra. J Am Soc Mass Spectrom. 1998; 9:225–233. [PubMed: 9879360]
37. Pascal BD, Chalmers MJ, Busby SA, Griffin PR. HD desktop: an integrated platform for the analysis and visualization of H/D exchange data. J Am Soc Mass Spectrom. 2009; 20:601–610. [PubMed: 19135386]
38. Bai Y, Milne JS, Mayne L, Englander SW. Primary structure effects on peptide group hydrogen exchange. Proteins. 1993; 17:75–86. [PubMed: 8234246]
39. Beckett D. Hydrogen-deuterium exchange study of an allosteric energy cycle. Methods Mol Biol. 2012; 796:261–278. [PubMed: 22052495]
40. Laine O, Streaker ED, Nabavi M, Fenselau CC, Beckett D. Allosteric signaling in the biotin repressor occurs via local folding coupled to global dampening of protein dynamics. J Mol Biol. 2008; 381:89–101. [PubMed: 18586268]

41. Li J, Dangott LJ, Fitzpatrick PF. Regulation of phenylalanine hydroxylase: conformational changes upon phenylalanine binding detected by hydrogen/deuterium exchange and mass spectrometry. Biochemistry. 2010; 49:3327–3335. [PubMed: 20307070]
42. Frantom PA, Zhang HM, Emmett MR, Marshall AG, Blanchard JS. Mapping of the allosteric network in the regulation of alpha-isopropylmalate synthase from Mycobacterium tuberculosis by the feedback inhibitor L-leucine: solution-phase H/D exchange monitored by FT-ICR mass spectrometry. Biochemistry. 2009; 48:7457–7464. [PubMed: 19606873]
43. Zawadzki KM, Hamuro Y, Kim JS, Garrod S, Stranz DD, Taylor SS, Woods VL Jr. Dissecting interdomain communication within cAPK regulatory subunit type IIbeta using enhanced amide hydrogen/deuterium exchange mass spectrometry (DXMS). Protein Sci. 2003; 12:1980–1990. [PubMed: 12930997]
44. Li S, Tsalkova T, White MA, Mei FC, Liu T, Wang D, Woods VL Jr, Cheng X. Mechanism of intracellular cAMP sensor Epac2 activation: cAMP-induced conformational changes identified by amide hydrogen/deuterium exchange mass spectrometry (DXMS). J Biol Chem. 2011; 286:17889–17897. [PubMed: 21454623]
45. Brudler R, Gessner CR, Li S, Tyndall S, Getzoff ED, Woods VL Jr. PAS domain allostery and light-induced conformational changes in photoactive yellow protein upon I2 intermediate formation, probed with enhanced hydrogen/deuterium exchange mass spectrometry. J Mol Biol. 2006; 363:148–160. [PubMed: 16952373]
46. Hochrein JM, Lerner EC, Schiavone AP, Smithgall TE, Engen JR. An examination of dynamics crosstalk between SH2 and SH3 domains by hydrogen/deuterium exchange and mass spectrometry. Protein Sci. 2006; 15:65–73. [PubMed: 16322569]
47. McAlister-Henn L. Ligand binding and structural changes associated with allostery in yeast NAD(+)-specific isocitrate dehydrogenase. Arch Biochem Biophys. 2011
48. Bloom CR, Kaarsholm NC, Ha J, Dunn MF. Half-site reactivity, negative cooperativity, and positive cooperativity: quantitative considerations of a plausible model. Biochemistry. 1997; 36:12759–12765. [PubMed: 9335532]
49. Ikeda Y, Tanaka T, Noguchi T. Conversion of non-allosteric pyruvate kinase isozyme into an allosteric enzyme by a single amino acid substitution. J Biol Chem. 1997; 272:20495–20501. [PubMed: 9252361]
50. Ikeda Y, Taniguchi N, Noguchi T. Dominant negative role of the glutamic acid residue conserved in the pyruvate kinase M(1) isozyme in the heterotropic allosteric effect involving fructose-1,6-bisphosphate. J Biol Chem. 2000; 275:9150–9156. [PubMed: 10734049]
51. Lipchock JM, Loria JP. Nanometer propagation of millisecond motions in V-type allostery. Structure. 2010; 18:1596–1607. [PubMed: 21134639]
52. Petit CM, Zhang J, Sapienza PJ, Fuentes EJ, Lee AL. Hidden dynamic allostery in a PDZ domain. Proc Natl Acad Sci U S A. 2009; 106:18249–18254. [PubMed: 19828436]
53. Zhang L, Bouguet-Bonnet S, Buck M. Combining NMR and Molecular Dynamics Studies for Insights into the Allostery of Small GTPase-Protein Interactions. Methods Mol Biol. 2012; 796:235–259. [PubMed: 22052494]

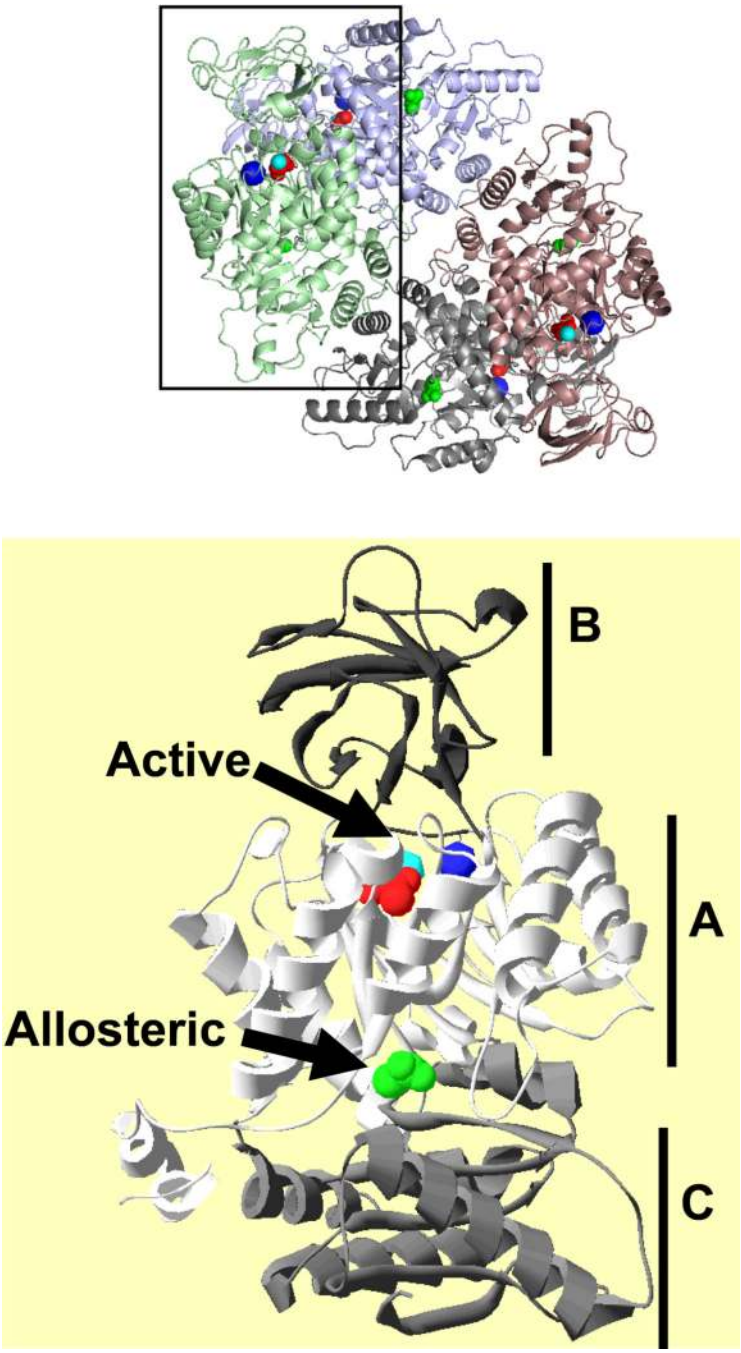

Figure 1.

The homotetrameric (top) and subunit (bottom) structures of rM_1-PYK as determined by X-ray crystallography (2G50). Subunits within the homotetramer are colored red, light blue, green and grey. Each subunit contains three domains labeled as A, B, and C. The active site lies between the A and B domains, whereas the amino acid allosteric site is located at the A/C domain interface. The presentation of the subunit (bottom) distinguishes the three domains with various shades of gray. In both homotetrameric and subunit views, the active site is occupied by spacefill views of potassium (blue), Mn^{2+} (cyan), and pyruvate (red). The allosteric amino acid binding site is occupied by alanine (green spacefill).

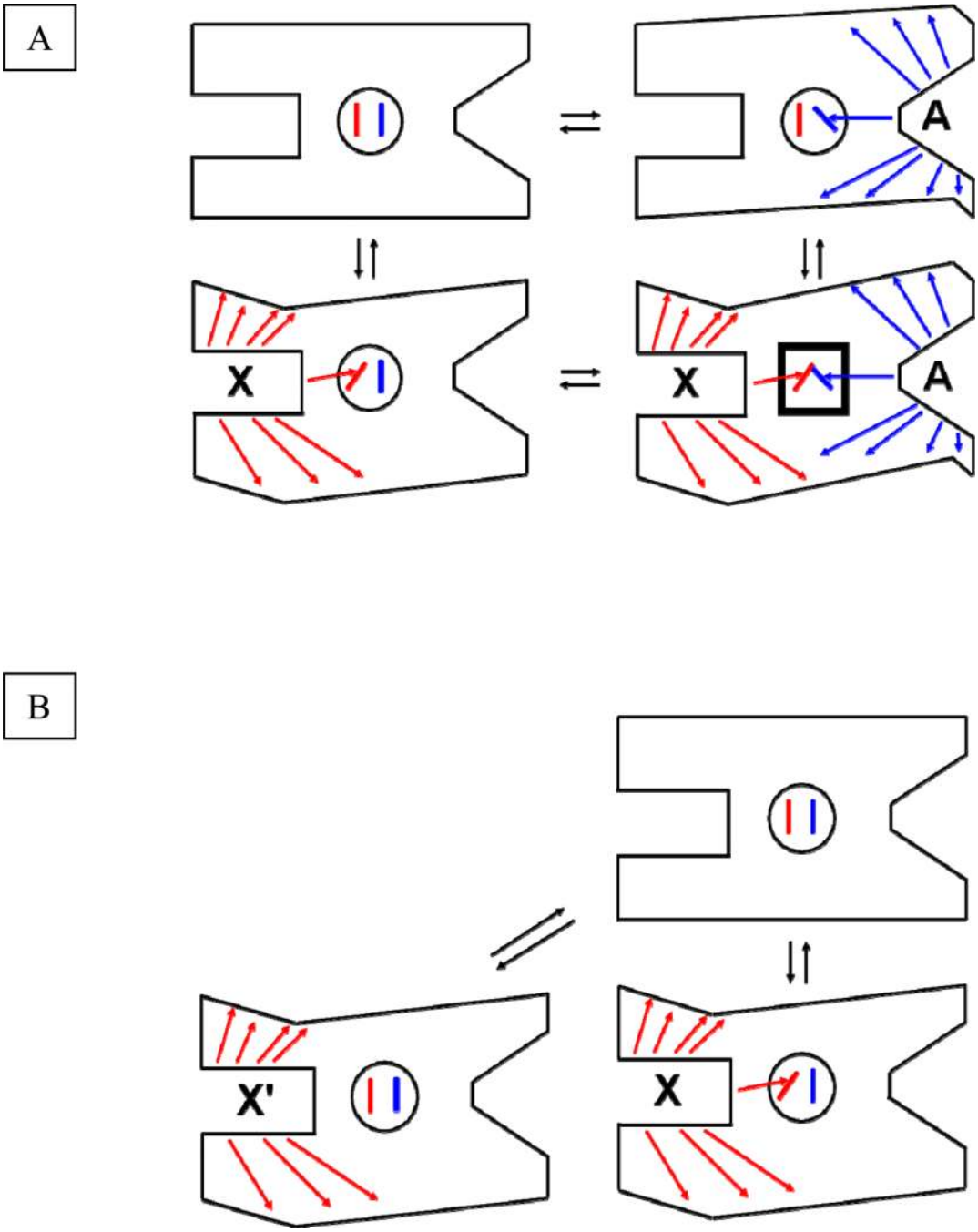

Figure 2.

A) Schematic representations of the four enzyme complexes in the allosteric energy cycle. B) Schematic representations of the complexes compared in this study. The box-like structure represents the protein. Substrate (PEP), allosteric effector (phenylalanine) and the non-allosteric effector analogue (alanine) are represented by A, X, and X', respectively. Changes in the proteins (whether conformational or dynamic) are represented by arrows and the outline of the protein. Many of the changes in the protein may have no relevance to allostery. The allosterically relevant changes are represented by shifting levers in the center of the protein. Adapted from (22).

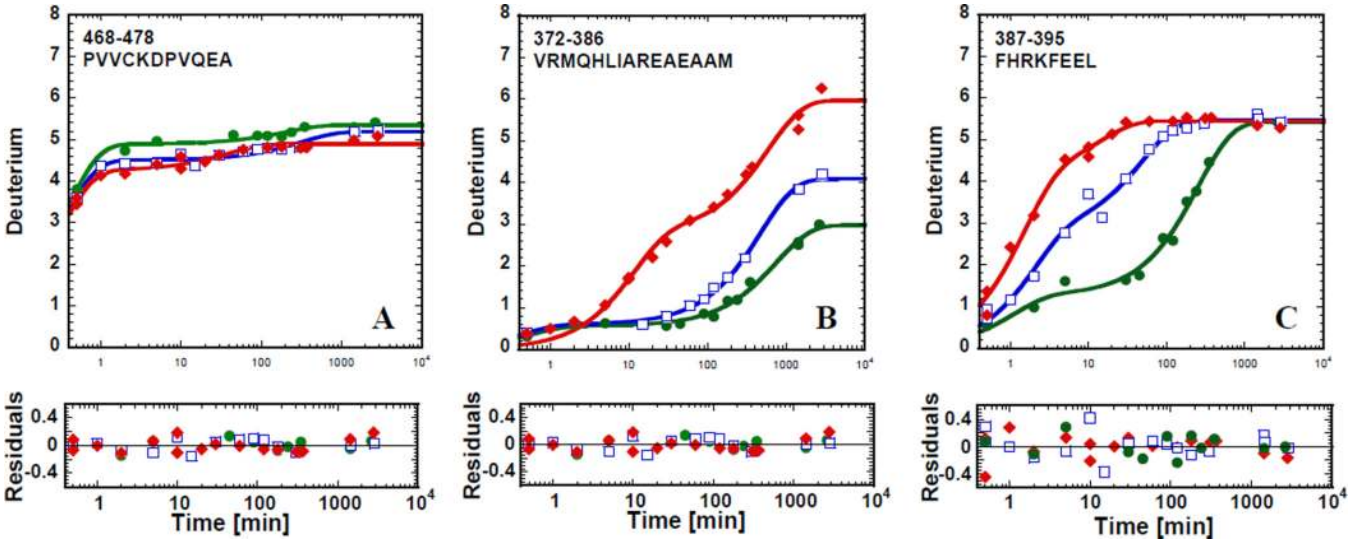

Figure 3.

Representative H/D-exchange of peptides from rM_1-PYK. Green (solid circle), blue (open square), and red (solid diamond) curve represents the free enzyme, the alanine-bound complex, and the phenylalanine-bound complex, respectively. Panel A represents a peptide which has similar response in all three complexes. Panel B represents a peptide which has different amount of deuterium incorporation upon binding either alanine or phenylalanine. Panel C represents a peptide which has similar amount of deuterium incorporation, but with different rates of exchange depending on which ligand is present. For each peptide in each complex the mass in protonated buffer (t=0) is included in the fit but is not shown in the graph.

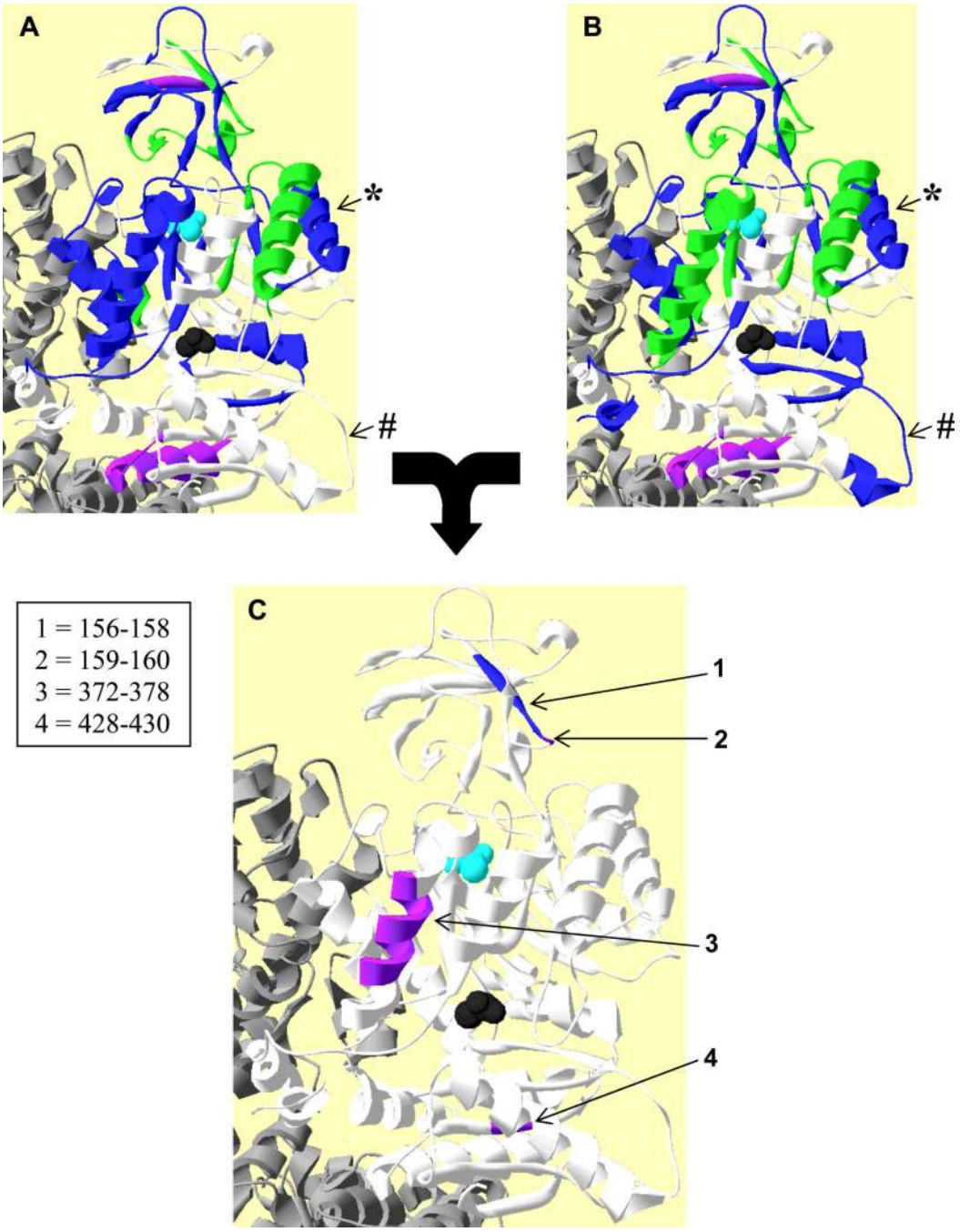

Figure 4.

Peptides/"units" in a subunit that have differences in the number of exchangeable protons depending on whether alanine or phenylalanine is bound. A) Differences highlighted by comparing the alanine-bound complex with the free enzyme. B) Differences highlighted by comparing the phenylalanine-bound complex with the free enzyme. C) Differences between the alanine-bound and phenylalanine-bound complexes. In all three panels, peptides with a difference of one proton are highlighted in blue, those with two are in purple and those with more than two are in green. These changes are mapped onto a subunit form the rM_1-PYK structure (2G50). Although only peptides detected by mass spectrometry are considered in the mapping in A and B, in C overlapping peptides were used to more precisely locate the

residues undergoing exchange (See Supplemental Figure S10). Neighboring subunits within the tetramer are in gray ribbon. Pyruvate in active site and alanine in the effector site are in cyan and black spacefill, respectively. An asterisk (*: peptide 215–237) and a pound symbol (#: 468–485) marks two helices discussed the text. Numbers denote locations of residue "units" that contain exchangeable protons that have changes associated with allostery (See Supplemental Figure S10).

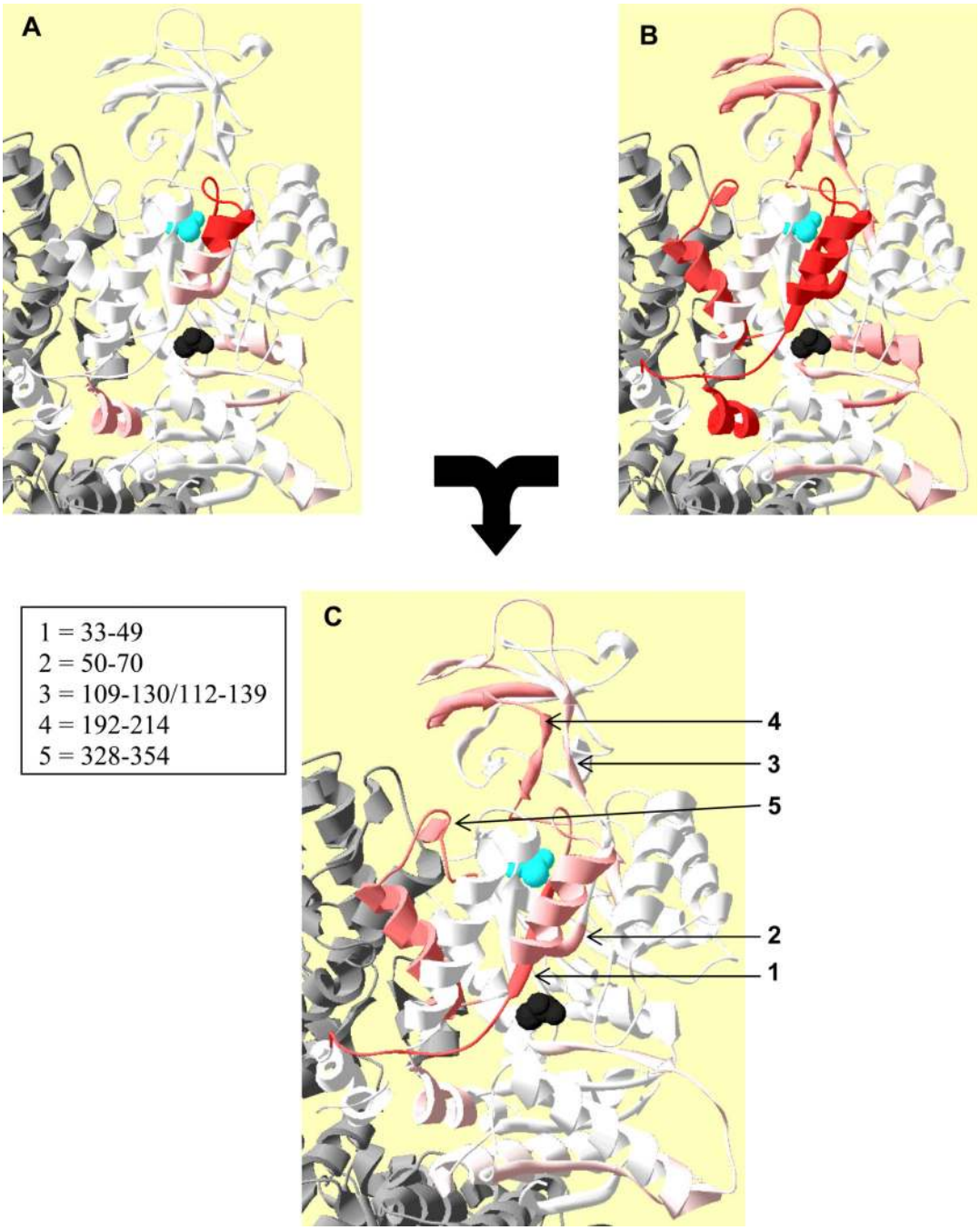

Figure 5.

Relative rate changes for proton exchange based on comparisons of identical peptides isolated from the various complexes. A) Differences highlighted by comparing the alanine-bound complex with the free enzyme. B) Differences highlighted by comparing the phenylalanine-bound complex with the free enzyme. C) Differences between the alanine-bound and phenylalanine-bound complexes. In panels A and B, the white to red gradient shows an increase in rates in the effector bound complex compared to the free enzyme. In panel C, the white to red gradient shows an increase in rates in the phenylalanine-bound complex compared to the alanine-bound complex (i.e. areas highlighted in red reflect regions of the protein that undergo faster exchange when phenylalanine is bound as

compared to when alanine is bound.) Differences in all panels have been scaled to the maximal change detected between the phenylalanine and alanine complexes. As a result, the color scale for rate differences are the same in all panels; changes in panel A and B that exceed the greatest change in panel C are in maximum red. Neighboring subunits within the tetramer are in grey ribbon. Pyruvate in active site and alanine in the effector site are in cyan and black spacefill, respectively. Numbers have been added as reference points for discussion.

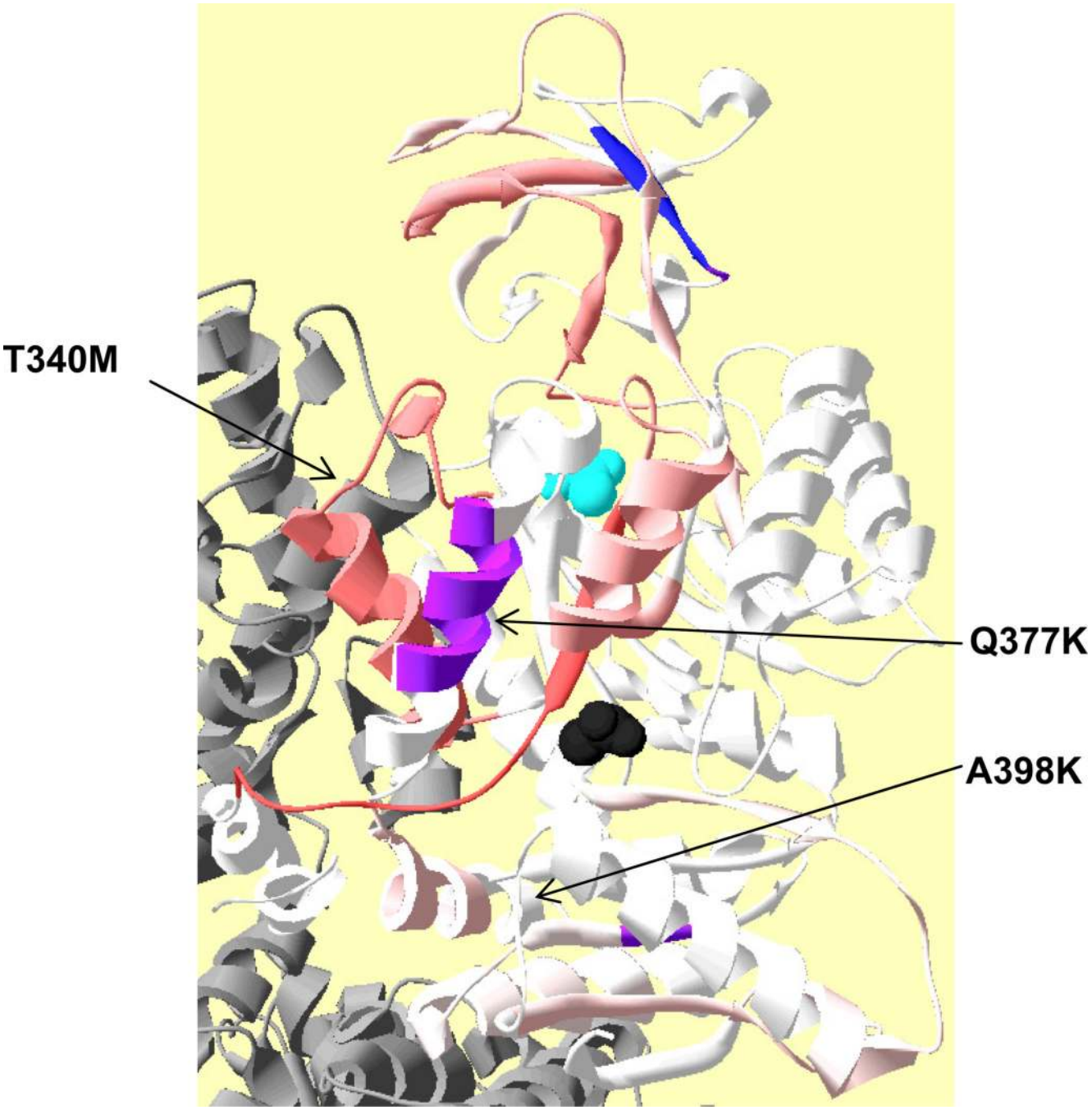

Figure 6.
A composite representation of all peptides highlighted with allosterically relevant changes, whether due to a change in the number of exchangeable protons (blue and purple; from Figure 4C) or due to a change in the rate of exchange (white to red gradient; from Figure 5C). The locations of three mutations known to alter allosteric regulation by phenylalanine are indicated.